Robust carrier formation process in low-band gap organic photovoltaics

Kouhei Yonezawa, Hayato Kamioka, Takeshi Yasuda, Liyuan Han, and Yutaka Moritomo
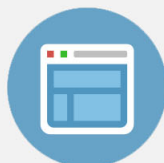
Robust carrier formation process in low-band gap organic photovoltaics

Kouhei Yonezawa,[1] Hayato Kamioka,[1,2] Takeshi Yasuda,[3] Liyuan Han,[3] and Yutaka Moritomo[1,2,a)]

[1]*Graduate School of Science and Engineering, University of Tsukuba, Tsukuba 305-8571, Japan*
[2]*Tsukuba Research Center for Interdisciplinary Materials Science (TIMS), University of Tsukuba, Tsukuba 305-8571, Japan*
[3]*Photovoltaic Materials Unit, National Institute for Materials Science (NIMS), Tsukuba 305-0047, Japan*

By means of femto-second time-resolved spectroscopy, we investigated the carrier formation process against film morphology and temperature (T) in highly-efficient organic photovoltaic, poly[[4,8-bis[(2-ethylhexyl)oxy]benzo[1,2-b:4,5-b'] dithiophene-2,6-diyl][3-fluoro-2-[(2-ethylhexyl) carbonyl]thieno[3,4-b] thiophenediyl]] (PTB7)/[6,6]-phenyl C_{71}-butyric acid methyl ester ($PC_{70}BM$) solar cells. We found that the carrier formation efficiency (ϕ_{CF}) from an absorbed photon is nearly independent of the film morphology, indicating that the internal quantum efficiency (ϕ_{IQ}) is mainly governed by the carrier transfer efficiency (ϕ_{CT}) to the electrodes. The activation energy ($E_a = 0.5$–0.8 meV) of ϕ_{CF} is significantly low, which suggests an extended charge-transfer state around the PTB7/$PC_{70}BM$ interface. © *2013 AIP Publishing LLC*. [http://dx.doi.org/10.1063/1.4826187]

Organic photovoltaic (OPV) with bulk heterojunction (BHJ)[1,2] is a promising energy conversion device with flexibility and low-cost production process, e.g., the roll-to-roll process. The BHJ active layer, where absorbed photons are converted into carriers, is the mixture of a nano level of donor (D) polymers and acceptor (A) molecules. In typical OPV, the active layer is sandwiched between an indium tin oxide (ITO) transparent anode and an Al cathode. Recently, Yu and coworkers have developed a series of low-band gap donor polymers based on alternating ester-substituted thieno[3,4-b]thiophene and benzodithiophene units (PTB n: $n = 1$–7).[3–5] The usage of the low-band gap donor polymer has increased the power conversion efficiency (PCE) of the OPV to ∼7–9%.[3,6,7] The increase in PCE stimulates extensive spectroscopic investigations of low-band gap blend films.[8–12] For example, Yonezawa *et al.*[11,12] reported fast exciton-to-carrier conversion process ($\tau = 0.2$–0.3 ps) in poly[[4,8-bis[(2-ethylhexyl)oxy]benzo[1,2-b:4,5-b'] dithiophene-2,6-diyl][3-fluoro-2-[(2-ethylhexyl)carbonyl]thieno [3,4-b] thiophenediyl]] (PTB7)/[6,6]-phenyl C_{71}-butyric acid methyl ester ($PC_{70}BM$) blend film.

The generation of the photocurrent in such OPV follows multi-step processes, i.e., (i) photogeneration of an exciton, (ii) exciton migration to the D/A interface, (iii) carrier formation via exciton dissociation, (iv) carrier transport within the D and A domains, and (v) collection of the carriers at the electrodes. We tentatively classify the processes into the carrier formation [(i)–(iii)] and the carrier transfer [(iv) and (v)] processes, because the former completes within several ps, while the latter requires much longer time ($\geq \mu$s). With this classification, the internal quantum efficiency (ϕ_{IQ}) is expressed as $\phi_{CF} \times \phi_{CT}$, where ϕ_{CF} and ϕ_{CT} are the carrier formation efficiency from an absorbed photon and the carrier transfer efficiency to the electrode. It is well-known that the ϕ_{IQ} value crucially depends on the film fabrication conditions, such as solvent, annealing temperature, and additive, via the modification of the film morphology.[13,14]

In this letter, we performed femto-second time-resolved spectroscopy on PTB7/$PC_{70}BM$ blend films against film morphology and temperature (T). The spectroscopy revealed that the ϕ_{CF} value is nearly independent of the film morphology, indicating that the ϕ_{IQ} value is mainly governed by the carrier transfer process to the electrodes. In addition, the activation energy ($E_a = 0.5$–0.8 meV) of ϕ_{CF} is much lower than the coulombic binding energy (∼100 meV) of a localized charge-transfer state. This suggests an extended charge-transfer state around the PTB7/$PC_{70}BM$ interface.

We fabricated a PTB7/$PC_{70}BM$ device in the following configuration:[15] ITO/poly(3,4-ethylenedioxythiophene) (PEDOT): poly(styrenesulfonate) (PSS) (40 nm)/active layer/LiF (1 nm)/Al (80 nm). PTB7 was purchased from 1-material Chemscitech, Inc., and used as received. The patterned ITO (conductivity: 10 Ω/square) glass was pre-cleaned in an ultrasonic bath of acetone and ethanol and then treated in an ultraviolet-ozone chamber. A thin layer (40 nm) of PEDOT: PSS was spin-coated onto the ITO and dried at 110 °C for 10 min on a hot plate in air. The substrate was then transferred to an N_2 glove box and dried again at 110 °C for 10 min on a hot plate. A mixed solvent of o-dichlorobenzene (o-DCB)/1,8-diiodooctane (DIO) (97.5: 2.5 vol. %) of PTB7: $PC_{70}BM$ with a ratio of 2:3 by weight (8:12 mg/ml) subsequently spin-coated onto the PEDOT: PSS surface to form the active layer. The spin-coated film was dried in an inert N_2 atmosphere. Finally, LiF (1 nm) and Al (80 nm) were deposited onto the active layer by conventional thermal evaporation at a chamber pressure lower than 5×10^{-4} Pa. The active area of the solar cell was 25 mm². For comparison, we fabricated another PTB7/$PC_{70}BM$ device from a chloroform (CF) solution of PTB7: $PC_{70}BM$ with a ratio of 2: 3 by weight (4: 6 mg/ml). For drastically changing of the film morphology and the performance of the device, we chose the solvents with different boiling-points:
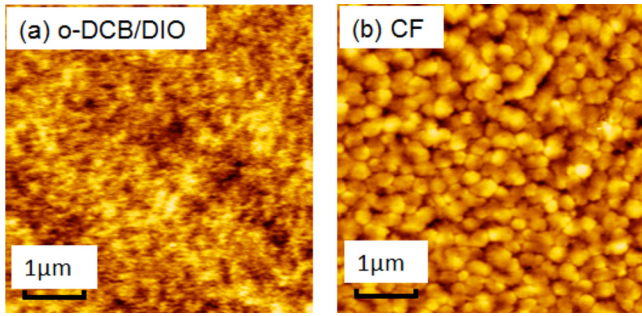
a)moritomo.yutaka.gf@u.tsukuba.ac.jp

FIG. 1. AFM images of PTB7/PC$_{70}$BM blend films made from (a) *o*-DCB/DIO (97.5: 2.5 vol. %) and (b) CF solvents.

TABLE I. Open circuit voltage (V_{oc}), short circuit current density (J_{sc}), FF, and PCE for the *o*-DCB/DIO and CF devices. PCE is expressed as $J_{sc} \times V_{oc} \times FF/I_0$, where I_0 is the power density of the incident light.

Solvent	V_{oc} (V)	J_{sc} (mA/cm^2)	FF (%)	PCE (%)
o-DCB/DIO	0.72	14.21	61	6.24
CF	0.76	7.34	42	2.32

CF with low boiling-point (61 °C) and *o*-DCB/DIO with high boiling-point (181 °C for *o*-DCB and 167 °C for DIO). Figure 1 shows AFM images of the active layers of (a) *o*-DCB/DIO and (b) CF devices. The domain size (∼100 nm) of the CF device is much larger than that of the *o*-DCB/DIO device. The thicknesses of the active layers of the *o*-DCB/DIO and CF devices were 107 and 98 nm, respectively.

Figure 2(a) shows current density-voltage (*J*–*V*) curves of the *o*-DCB/DIO and CF devices. The curves were measured using a voltage current source/monitor under AM 1.5 solar-simulated light irradiation of 100 mW/cm^2 (Bunkou-keiki, OTENTO-SUN III). In Table I, we summarized performances, i.e., the open circuit voltage (V_{oc}), short circuit current density (J_{sc}), fill factor (FF), and PCE of the *o*-DCB/DIO and CF devices. Figure 2(b) shows absorption coefficients (α) of the blend films. The spectral feature and absolute magnitude of α are almost mutually the same. The absorption edge is ∼750 nm. Figure 2(c) shows incident photon to current conversion efficiency (IPCE) spectra of the devices, which was measured using a SM-250 system (Bunkou-keiki). The magnitudes of IPCE at 400 nm for the *o*-DCB/DIO and CF devices are 0.55 and 0.34, respectively. Considering the absorbed photon density within the active layers, the magnitudes of ϕ_{IQ} at 400 nm are estimated to be 0.87 and 0.51, respectively. The lower ϕ_{IQ} value of the CF device is ascribed to the larger domain size [see Fig. 1(b)], which may be disadvantageous for both the carrier formation (ϕ_{CF}) and the carrier transfer (ϕ_{CT}) processes. Here, we
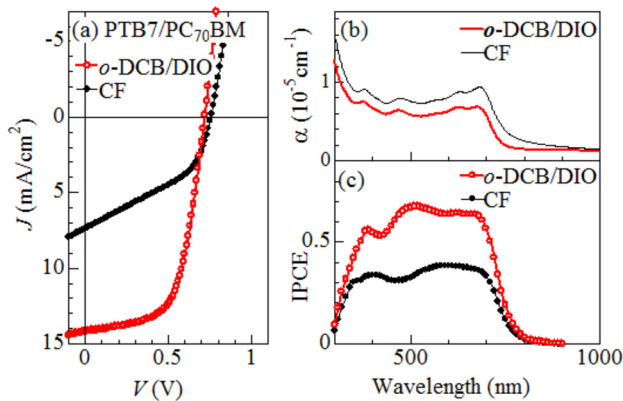
emphasize that the femto-second time-resolved spectroscopy is a powerful tool to distinguish the two processes in the time domain.

For the time-resolved spectroscopy, the PTB7/PC$_{70}$BM blend films were spin-coated on quartz substrates from *o*-DCB/DIO and CF solvents and were dried in an inert N$_2$ atmosphere. The thicknesses of the blend films made from *o*-DCB/DIO and CF solutions were 140 and 81 nm, respectively. The time-resolved spectroscopy[12] was carried out in a pump-probe configuration against *T*. The blend film was placed on a cold head of a cryostat, whose temperature was controlled with a liquid nitrogen. The wavelength of the pump pulse was 400 nm, which was generated as second harmonics of a regenerative amplified Ti:sapphire laser in a β-BaB$_2$O$_4$ (BBO) crystal. The pulse width and repetition rate are 100 fs and 1000 Hz, respectively. The excitation intensity (I_{ex}) was 27 μJ/cm^2. We confirmed that the signal intensity is proportional to I_{ex}. The frequency of the pump pulse was decreased by half (500 Hz) to provide "pump-on" and "pump-off" condition. The white probe pulse (450–1600 nm), generated by self-phase modulation in a sapphire plate, was focused on the sample with the pump pulse. The spot sizes of the pump and probe pulses were 4.2 and 2.0 mm in diameter, respectively. The transmitted probe spectra were detected using a 256 ch InGaAs photodiode array (800–1600 nm) attached to a 30 cm imaging spectrometer. The spectral data were accumulated for 20 000–50 000 pulses to improve the signal/noise ratio. The differential absorption spectra (ΔOD) is expressed as $\Delta OD \equiv -\log(\frac{I_{on}}{I_{off}})$, where I_{on} and I_{off} are the transmission spectra under the "pump-on" and "pump-off" conditions, respectively. The time resolution of the system is ∼0.3 ps.

Figure 3(a) shows the ΔOD spectrum for the PTB7/PC$_{70}$BM blend film made from *o*-DCB/DIO solvent. The spectrum exhibits positive broad signal centered at 1174 nm. The positive signal is ascribed to the photoinduced absorption (PIA) due to the holes on the donor polymer.[8,11,12] Actually, the ΔOD spectrum resembles the optical modulation spectra of the PTB7 neat film.[11,12] In the earlier stage (≤0.3 ps) after photo excitation, the hole component of the PIA is overlapped by the exciton component.[8,11,12] The spectral profile is essentially unchanged above 0.6 ps, indicating that the PIA consists of only the hole component. Figure 3(c) shows signal intensity (*I*) at 1174 nm against time at 300 K. The magnitude of *I* steeply increases within the time resolution of the system, and then gradually increases with time. Figures 3(b) and 3(d) show the ΔOD spectrum and the time dependence of *I* for the film made from CF solvent. Their features are similar to those of the film made from *o*-DCB/DIO solvent [Figs. 3(a) and 3(c)], indicating that the PIA is ascribed to the holes on the donor polymer.

FIG. 2. (a) Current density-voltage (*J* − *V*) curves of PTB7/PC$_{70}$BM solar cells made from *o*-DCB/DIO and CF solvents. (b) Absorption coefficients (α) of PTB7/PC$_{70}$BM blend films made from *o*-DCB/DIO and CF solvents. (c) IPCE spectra of the *o*-DCB/DIO and CF devices.
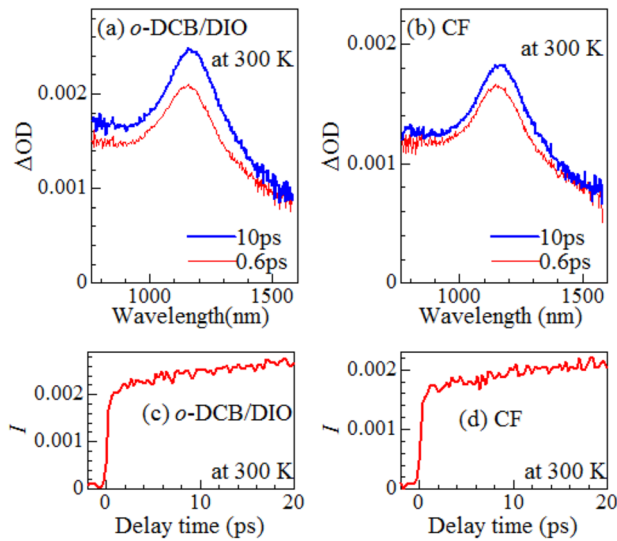
FIG. 3. Time dependence of ΔOD at 300 K for PTB7/PC$_{70}$BM blend films made from (a) *o*-DCB/DIO and (b) CF solvents. Signal intensity (I) at 1174 nm against time at 300 K for the PTB7/PC$_{70}$BM blend films made from (c) *o*-DCB/DIO and (d) CF solvents.

Now, let us compare the magnitudes of ϕ_{CF}, which are defined by the generated carrier number per an absorbed photon, between the two blend films. In the present experiment, the absorbed photon densities (n) are 3.3×10^{13} and 2.7×10^{13} cm^{-2} for the films made from *o*-DCB/DIO and CF solvents, respectively. Unfortunately, we cannot estimate the absolute value of ϕ_{CF} since we have no information on the oscillator strengths of the PIA per hole. We tentatively estimate the I/n value, which is proportional to ϕ_{CF}. In Table II, we summarize ϕ_{CF}, ϕ_{CT}, and ϕ_{IQ} for the two devices. Our time-resolved spectroscopy revealed that the ϕ_{CF} values are mutually the same ($\equiv \phi_0$). Surprisingly, the exciton migration within the domain causes negligible loss even in the CF device with large domains [Fig. 1(b)]. The negligible loss is probably originated in the fast carrier formation time ($\tau = 0.2$–0.3 ps)[11,12] as well as the highly-efficient exciton dissociation process within the BHJ active layer. On the other hand, the ϕ_{CT} value is much suppressed in the CF device. The significant loss is ascribed to the slow carrier transfer process ($\geq \mu$s) and resultant carrier recombination and/or trapping.

Next, let us discuss on the temperature effect on the carrier formation process. In the exciton migration process, the migration suffers from the potential distribution due to the bending and crossing of the polymer backbone. In the exciton dissociation process, the dissociation suffers from the

TABLE II. Internal quantum efficiency (ϕ_{IQ}), carrier formation efficiency (ϕ_{CF}) per an absorbed photon, carrier transfer efficiency (ϕ_{CT}) to the electrode per a produced carrier for PTB7/PC$_{70}$BM solar cells made from *o*-DCB/DIO and CF solvents. The time-resolved spectroscopy revealed that the ϕ_{CF} values are almost mutually the same ($\equiv \phi_0$). ϕ_{CT} is expressed as ϕ_{IQ}/ϕ_{CF}.

Solvent	ϕ_{IQ}	ϕ_{CF}	ϕ_{CT}
o-DCB/DIO	0.87	ϕ_0	$0.87/\phi_0$
CF	0.51	ϕ_0	$0.51/\phi_0$

strong coulombic binding energy between the constituent electron and hole. The coulombic binding energy is several hundred meV,[16,17] if the electron and hole localize on the adjacent molecules at the interface (charge-transfer state). Such charge-transfer states are frequently observed in poly(3-hexylthiophene) (P3HT)/[6,6]-phenyl C$_{61}$-butyric acid methyl ester (PCBM) interface[18] and α-sexithiophene (6 T)/C$_{60}$ interface.[19] Here, we propose that the coulombic binding energy of the charge-transfer state is detectable as the activation energy (E_a) of ϕ_{CF}.

Figure 4(a) shows temperature dependence of the ΔOD spectrum at 10 ps for the PTB7/PC$_{70}$BM blend film made from *o*-DCB/DIO solvent. The spectral weight slightly increases with T, reflecting the thermal activation behavior of the exciton dissociation process. Figure 4(c) shows the Arrhenius plot of I at 1174 nm against inverse temperatures. To precisely estimate the mean values and standard deviations of I, the time-resolved measurements were performed at eight different positions of the film at each temperature. The E_a value is estimated to be 0.8 ± 0.2 meV [straight line in Fig. 4(b)]. A similar thermal activation behavior of I is observed in the blend film made from CF solvent [Figs. 4(b) and 4(d)]. The E_a value is estimated to be 0.5 ± 0.1 meV. The smaller E_a value of the CF device perhaps reflects more homogeneous D/A interface. Here, we emphasize that thus-evaluated E_a values (=0.5–0.8 meV) are much smaller than the expected coulombic binding energy ($\sim$100 meV) of a localized charge-transfer state. In addition, the E_a values of ϕ_{CF} are much smaller than that (=100 meV) of the external quantum efficiency in PTB7/PCBM blend film.[20]

The small E_a value suggests an extended charge-transfer state at the PTB7/PC$_{70}$BM interface, which reduces the coulombic binding energy between the electron and hole. By means of *ab initio* calculation, Kanai and Grossman[21] investigated the charge-transfer state at the P3HT/C$_{60}$ interface, and observed an extended charge-transfer state. The state has
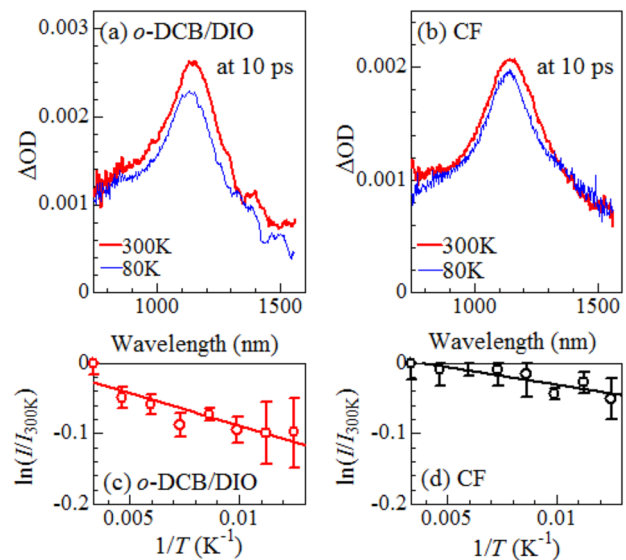

FIG. 4. Temperature dependence of ΔOD spectrum at 10 ps for PTB7/PC$_{70}$BM blend films made from (a) *o*-DCB/DIO and (b) CF solvents. Arrhenius plot of signal intensity (I) at 1174 nm for PTB7/PC$_{70}$BM blend films made from (c) *o*-DCB/DIO and (d) CF solvents. The straight lines in (c) and (d) are the results of least-squares fitting.

a significant probability distribution across the interface and a significant overlap with the lowest-unoccupied molecular orbital (LUMO) state on C_{60}. We believe that a similar extended charge-transfer state is realized at the PTB7/$PC_{70}BM$ interface. Recently, Collins *et al.*[22] investigated the domain structure of PTB7/$PC_{70}BM$ blend film as well as the effect of the DIO additive. Their careful analysis revealed that the blend film consists of pure fullerene agglomerates (A domain) and a polymer-rich 70/30 wt. % molecularly mixed matrix (D domain). The addition of DIO drastically reduces the domain size, but has negligible effects on the composition and crystallinity of the domains. A similar molecular mixing is observed in naphtha[1,2–c:5,6-c] bis[1,2,5]thiadiazole (NT) material/fullerene derivative and 2,1,3-benzothiadiazole (BT) material/fullerene derivative blend films.[23] Such a molecular mixing in the D domain is advantageous for the extended charge-transfer state, because the electronic state of the D domain approaches to that of pure fullerene domain.

In conclusion, we performed femto-second time-resolved spectroscopy on PTB7/$PC_{70}BM$ blend films against film morphology and T. Quantitative analysis of the PIA signal revealed that the carrier formation process is fairly robust against the film morphology. The small E_a values ($=0.5$–0.8 meV) suggests an extended charge-transfer state at the PTB7/$PC_{70}BM$ interface.

[1] M. Hiramoto, H. Fujiwara, and M. Yokoyama, Appl. Phys. Lett. **58**, 1062 (1991).
[2] N. S. Sariciftci, L. Smilowitz, A. J. Heeger, and F. Wudl, Science **258**, 1474 (1992).
[3] Y. Liang, Z. Xu, J. Xia, S.-T. Tsai, Y. Wu, G. Li, C. Ray, and L. Yu, Adv. Mater. **22**, E135 (2010).
[4] Y. Liang and L. Yu, Acc. Chem. Res. **43**, 1227 (2010).
[5] Y. Liang, Y. Wu, D. Feng, S.-T. Tsai, H.-J. Son, G. Li, and L. Yu, J. Am. Chem. Soc. **131**, 56 (2009).
[6] Z. He, C. Zhong, S. Su, M. Xu, H. Wu, and Y. Cao, Nat. Photonics **6**, 593 (2012).
[7] Z. He, C. Zhong, X. Huang, W.-Y. Wong, H. Wu, L. Chen, S. Su, and Y. Cao, Adv. Mater. **23**, 4636 (2011).
[8] J. Guo, Y. Liang, J. Szarko, B. Lee, H.-J. Son, B. S. Rolczynski, L. Yu, and L. X. Chen, J. Phys. Chem. B **114**, 742 (2010).
[9] J. M. Szarko, J.-C. Guo, B. S. Rolczynski, and L. X. Chen, J. Mater. Chem. **21**, 7849 (2011).
[10] B. S. Rolczynski, J. M. Szarko, H. J. Son, Y. Liang, L. Yu, and L. X. Chen, J. Am. Chem. Soc. **134**, 4142 (2012).
[11] K. Yonezawa, H. Kamioka, T. Yasuda, L. Han, and Y. Moritomo, Appl. Phys. Express **5**, 042302 (2012).
[12] K. Yonezawa, H. Kamioka, T. Yasuda, L. Han, and Y. Moritomo, Jpn. J. Appl. Phys. Part 1 **52**, 062405 (2013).
[13] L. Bian, E. Zhu, J. Tang, W. Tang, and F. Zhang, Prog. Polym. Sci. **37**, 1292 (2012).
[14] M. T. Dang, L. Hirsch, and G. Wantz, Adv. Mater. **23**, 3597 (2011).
[15] T. Yasuda, Y. Shinohara, T. Ishi-i, and L. Han, Org. Electron. **13**, 1802 (2012).
[16] Y. Yi, V. Coropceanu, and J.-L. Brédas, J. Mater. Chem. **21**, 1479 (2011).
[17] Y. Yi, V. Coropceanu, and J.-L. Brédas, J. Am. Chem. Soc. **131**, 15777 (2009).
[18] I.-W. Hwang, D. Moses, and A. J. Heeger, J. Phys. Chem. C **112**, 4350 (2008).
[19] Y. Takahashi, K. Yonezawa, H. Kamioka, T. Yasuda, L. Han, and Y. Moritomo, J. Phys. Soc. Jpn. **82**, 063709 (2013).
[20] J. Tsutsumi, H. Matsuzaki, N. Kanai, T. Yamada, and T. Hasegawa, J. Phys. Chem. C **117**, 16769 (2013).
[21] Y. Kanai and J. C. Grossman, Nano Lett. **7**, 1967 (2007).
[22] B. A. Collins, Z. Li, J. R. Tumbleston, R. Gann, C. R. McNeill, and H. Ade, Adv. Energy Mater. **3**, 65 (2013).
[23] W. Ma, J. R. Tumbleston, M. Wang, E. Gann, F. Huang, and H. Ade, Adv. Energy Mater. **3**, 864 (2013).